AIAA JOURNAL
Vol. 44, No. 11, November 2006

Response and Control of Smart Laminates Using a Refined Hybrid Plate Model

P. Topdar,* A. H. Sheikh,† and N. Dhang‡
Indian Institute of Technology, Kharagpur, West Bengal 721 302, India

DOI: 10.2514/1.6467

The dynamic response of smart composite/sandwich laminates and its control is studied using a refined hybrid plate theory to model the coupled electromechanical field problem in the present study. The proposed plate model consists of a refined plate theory and layerwise theory for through-thickness representation of structural deformation (mechanical field) and electric potential, respectively. The refined plate theory has the elegance that it ensures interlaminar shear stress continuity as well as stress free conditions at the plate top and bottom surfaces with the unknowns at the reference plane only. To have any arbitrary through-thickness variation of electric potential due to the presence of embedded piezoelectric layers, the layerwise theory is used. Though it requires unknowns at all the interfaces, they are eliminated from the final system of equations. The in-plane variations of unknowns at the reference plane for structural deformation and those for the electric potential at the different interfaces are approximated by the finite element technique. As the proposed plate model requires C^1 continuity of transverse displacement at the element interfaces, a new rectangular element is developed where this requirement is fully ensured. Finally, numerical examples are solved to study the different aspects of the present problem.

Nomenclature

$\{f\}$	=	vector of displacement parameters at plate midplane
$\{f\}$	=	displacement field
h	=	overall thickness of the plate
n_l, n_u	=	number of layers below and above the midplane, respectively, of the laminated plate
u, v	=	in-plane displacements along x-direction and y-direction, respectively, at the midplane of the plate
$\bar{u}$, $\bar{v}$	=	in-plane displacements at any point
w	=	transverse displacement at the midplane of the plate
$w_{,x}$, $w_{,y}$	=	first partial derivative of w with respect to x and y, respectively
$\bar{w}$	=	transverse displacement at any point
α_x^i, α_y^i	=	change in slope at the i-th interface in the x and y directions, respectively
$\{\delta\}$	=	element displacement vector
$\{\varepsilon\}$	=	strain vector at the midplane of the plate
$\{\bar{\varepsilon}\}$	=	strain vector at any point of the plate
$\{\bar{\sigma}\}$	=	stress vector at any point of the plate

I. Introduction

A realistic prediction of the structural response of composite or sandwich laminates with embedded or surface-bonded piezoelectric layers is one of the challenging problems, as it requires modeling of a coupled electromechanical field problem in a layered media. For such a problem, the most common approach is due to Hagood et al. [1], Ray et al. [2,3], Kim et al. [4], and a few others where the piezoelectric layers are essentially surface-bonded and the interface of these layers with the core is grounded to make the electric potential zero over the entire core. It leads to a simple through-thickness variation of electric potential, which may be represented by two unknowns (at the plate top and bottom surfaces) taking linear variation of potential across the piezoelectric layers. In these studies, the structural deformation is represented by a plate model based on the single layer theory (SLT), such as classical plate theory, first-order shear deformation theory (FSDT), and higher order shear deformation theory (HSDT). These models are definitely simple and easy to implement but they are not capable enough to model a complex problem. A major limitation of these models is that piezoelectric layers cannot be embedded inside the plate and through-thickness variation of potential cannot be made arbitrary. Moreover, these plate models are not competent enough for accurate prediction of stresses. In the case of sandwich laminates, they are not suitable even for the evaluation of global parameters like displacement, natural frequency, or buckling load.

In this context, the other extreme is due to Allik and Hughes [5], Tzou and Tseng [6], Sze and Yao [7], and a few others who have used three-dimensional (3-D) finite element analysis to solve the problem. It is obvious that the 3-D analysis gives better accuracy and generality but it requires huge computational effort. The computational involvement becomes prohibitively high when piezoelectric layers are too thin compared with the plate dimensions, which is quite common in many practical problems. As a result, the 3-D finite element analysis may become unsuitable in handling a real problem. An improvement in this direction is due to Heyliger et al. [8,9] who have used layerwise theory (LWT) [10–13] instead of 3-D finite element modeling. In this approach LWT, the through-thickness variation of structural deformation, as well as electric potential, is represented by piecewise linear interpolation functions with unknowns at all the layer interfaces including plate top and bottom. Though the computational involvement in LWT is somewhat less compared with that in 3-D analysis, LWT may not be suitable for a multilayered plate, as the number of unknowns is dependent on the number of layers. To overcome this difficulty, Mitchell and Reddy [14], Saravanos [15], and Sheikh et al. [16] have proposed the concept of hybrid plate theory (HPT), where the structural deformation and the electrical field are modeled by SLT and LWT, respectively. With the use of SLT having unknowns at the reference plane only, HPT becomes computationally quite economic and generality of the problem is not affected. However, these hybrid models inherit the limitations of SLT in modeling layered plates as mentioned earlier.

In a layered plate like composite/sandwich laminate, the in-plane strains and out-of-plane stresses are continuous at the layer interfaces, whereas in-plane stresses and out-of-plane strains are discontinuous due to difference in the rigidities of the adjacent layers. In SLT, the variation of displacement components across the plate thickness is expressed by continuous functions. Consequently, all the

Received 14 November 2003; revision received 2 May 2006; accepted for publication 8 June 2006.

*Research Scholar, Department of Ocean Engineering and Naval Architecture.
†Associate Professor, Department of Ocean Engineering and Naval Architecture; Corresponding Author, E-mail: hamid@naval.iitkgp.ernet.in.
‡Associate Professor, Department of Civil Engineering.

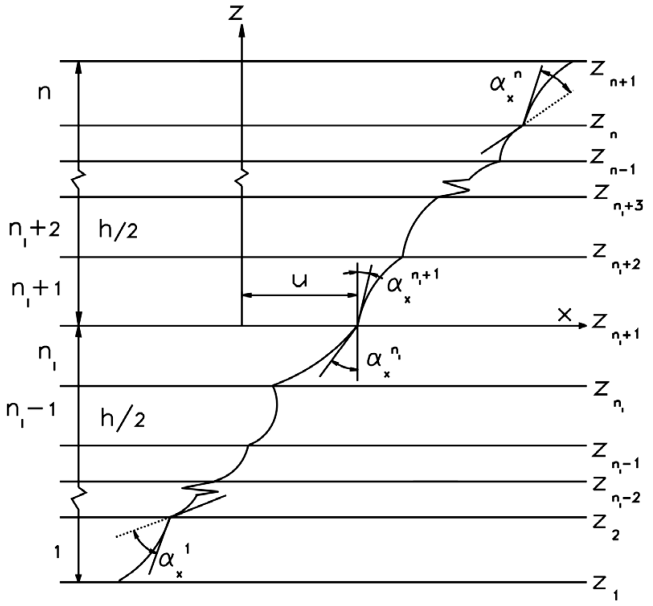

Fig. 1 General lamination configuration.

strain components become continuous and stress components become discontinuous at the layer interfaces. Thus, SLT cannot properly represent the out-of-plane deformation of layered plates. It is this drawback that has inspired researchers to develop LWT, however, this theory involves unknowns at all the interfaces as mentioned earlier.

To have the capability of LWT and computational economy of SLT, a refined plate theory is used to represent the through-thickness variation of structural deformation in the present study. The development of refined plate theories has been initiated by Di Sciuva [17], who has pioneered contribution to this field. This plate theory and some similar theories, such as that of Lue and Li [18] and a few others, are defined as refined first-order shear deformation theory (RFSDT). In RFSDT, the in-plane displacements have piecewise linear variation across the plate thickness like that of LWT, whereas transverse displacement is constant over the entire thickness. Such a variation of in-plane displacements is obtained by taking unknowns initially at all the interfaces like in LWT, but all these unknowns are ultimately replaced by some unknowns at the reference plane through satisfaction of transverse shear stress continuity at the layer interfaces. A further improvement over RFSDT is due to Bhaskar and Varadan [19], Di Sciuva [20], Lee and Liu [21], and Cho and Parmerter [22] who have combined the concepts of RFSDT and HSDT (third-order SLT) of Reddy [23] to develop another class of refined theory defined as refined higher order shear deformation theory (RHSDT). The theory gives piecewise parabolic variation of transverse shear stress across the plate thickness with continuity at the layer interfaces, which introduces transverse shear strain jumps at the layer interfaces as desired. Moreover, the transverse shear stresses become zero at the plate top and bottom surfaces in RHSDT. To embed the piezoelectric layers inside the plate and to have any suitable variation of potential across the plate thickness, the electric field is represented by the LWT, which involves unknowns at all the interfaces. This makes the size of the element matrices quite large at the beginning, but the size is drastically reduced by eliminating all the degrees of freedom for the electric potentials E_{DOF} through static condensation.

With the preceding plate model, the in-plane variation of unknowns is represented through finite element approximation. In this context, it should be noted that the present plate model demands C^1 continuity of w at the element interfaces, as it involves second-order derivatives of w in the strain components. This is a well-known problem of plate finite element, which is found in all the refined theories. Keeping this aspect in view, a new rectangular element is developed where the aforementioned continuity requirement is fully ensured by taking bicubic Hermitian polynomials for the interpolation of w. The other field variables are interpolated with bilinear interpolation functions. The details of the element are given in the section of mathematical formulation.

The performance of the proposed model is tested with numerical examples under static and dynamic conditions before it is applied to the final problem, where a number of results are generated to study the different aspects of the present problem.

II. Mathematical Formulation

According to RHSDT, the variation of in-plane displacements across the plate thickness (Fig. 1) may be expressed in terms of linearly varying zigzag components combined with a cubically varying continuous component as follows:

$$\bar{u} = u + \sum_{i=1}^{n_l} \alpha_x^i (z - z_{i+1}) H(-z + z_{i+1}) + \sum_{i=n_l+1}^{n_l+n_u} \alpha_x^i (z - z_i) \times H(z - z_i) + \beta_x z^2 + \eta_x z^3 \tag{1}$$

$$\bar{v} = v + \sum_{i=1}^{n_l} \alpha_y^i (z - z_{i+1}) H(-z + z_{i+1}) + \sum_{i=n_l+1}^{n_l+n_u} \alpha_y^i (z - z_i) \times H(z - z_i) + \beta_y z^2 + \eta_y z^3 \tag{2}$$

where H is the unit step function.

The transverse displacement is taken to be constant over the plate thickness and it may be expressed as

$$\bar{w} = w \tag{3}$$

According to layerwise theory, the through-thickness variation of electric potential may be expressed as

$$\phi = \sum_{i=1}^{n+1} \psi^i \phi^i \tag{4}$$

where ϕ^i is the potential at the ith interface, n is the total number of layers ($n_l + n_u$), and ψ^i is the piecewise linear function as follows:

$$\psi^i = (z - z_{i-1})/(z_i - z_{i-1})[H(z_i - z) - H(z_{i-1} - z)] + (z_{i+1} - z)/(z_{i+1} - z_i)[H(z_{i+1} - z) - H(z_i - z)] \tag{4a}$$

Assuming normal stress $\sigma_z = 0$, the constitutive equation of a piezoelectric lamina may be expressed in the structural axes system as

$$\begin{Bmatrix} \sigma_x \\ \sigma_y \\ \tau_{xy} \\ \tau_{xz} \\ \tau_{yz} \\ D_x \\ D_y \\ D_z \end{Bmatrix} = \begin{bmatrix} \bar{Q}_{11} & \bar{Q}_{12} & \bar{Q}_{16} & 0 & 0 & 0 & 0 & \bar{Q}_{91} \\ \bar{Q}_{12} & \bar{Q}_{12} & \bar{Q}_{26} & 0 & 0 & 0 & 0 & \bar{Q}_{92} \\ \bar{Q}_{16} & \bar{Q}_{26} & \bar{Q}_{66} & 0 & 0 & 0 & 0 & \bar{Q}_{93} \\ 0 & 0 & 0 & \bar{Q}_{55} & \bar{Q}_{45} & \bar{Q}_{75} & \bar{Q}_{74} & 0 \\ 0 & 0 & 0 & \bar{Q}_{45} & \bar{Q}_{44} & \bar{Q}_{74} & \bar{Q}_{84} & 0 \\ 0 & 0 & 0 & \bar{Q}_{75} & \bar{Q}_{74} & -\bar{Q}_{77} & -\bar{Q}_{78} & 0 \\ 0 & 0 & 0 & \bar{Q}_{74} & \bar{Q}_{84} & -\bar{Q}_{78} & -\bar{Q}_{88} & 0 \\ \bar{Q}_{91} & \bar{Q}_{92} & \bar{Q}_{93} & 0 & 0 & 0 & 0 & \bar{Q}_{99} \end{bmatrix} \begin{Bmatrix} \varepsilon_x \\ \varepsilon_y \\ \gamma_{xy} \\ \gamma_{xz} \\ \gamma_{yz} \\ -E_x \\ -E_y \\ -E_z \end{Bmatrix} \quad \text{or} \quad \{\bar{\sigma}\} = [\bar{Q}^k]\{\bar{\varepsilon}\} \tag{5}$$

where the different parameters in the rigidity matrix of the kth lamina $[\bar{Q}^k]$ can be obtained from material properties and fiber orientation of that lamina. The detailed derivation of these equations is available in an earlier study [24].

Using the condition of zero transverse shear stress at the plate top and bottom surfaces, β_x, β_y, η_x, and η_y may be expressed in terms of the other quantities of Eqs. (1–3) as

$$\beta_x = -\frac{1}{2h}\sum_{i=1}^{n}\alpha_x^i, \qquad \beta_y = -\frac{1}{2h}\sum_{i=1}^{n}\alpha_y^i$$

$$\eta_x = -\frac{4}{3h^2}\left[w_{,x} - \frac{1}{2}\sum_{i=1}^{n_l}\alpha_x^i + \frac{1}{2}\sum_{i=n_l+1}^{n}\alpha_x^i\right] \quad \text{and} \tag{6a}$$

$$\eta_y = -\frac{4}{3h^2}\left[w_{,y} - \frac{1}{2}\sum_{i=1}^{n_l}\alpha_y^i + \frac{1}{2}\sum_{i=n_l+1}^{n}\alpha_y^i\right]$$

Now, imposing the condition of transverse shear stress continuity at the interfaces between the layers, α_x^i and α_y^i may be finally expressed in terms of the quantities at the reference plane as

$$\begin{aligned}\alpha_x^i &= a_{xx}(\gamma_x) + a_{xy}(\gamma_y) + b_{xx}w_{,x} + b_{xy}w_{,y}\\ \alpha_y^i &= a_{yx}(\gamma_x) + a_{yy}(\gamma_y) + b_{yx}w_{,x} + b_{yy}w_{,y}\end{aligned} \tag{6b}$$

where $\gamma_x(=w_{,x} - \theta_x = w_{,x} + \alpha_x^{n_l+1})$ and $\gamma_y(=w_{,y} - \theta_y = w_{,y} + \alpha_y^{n_l+1})$ are the transverse shear strains at the reference plane, whereas the constants $(a_{xx}, a_{xy}, b_{xx}, b_{yy}, \ldots)$ are dependent on the material properties of the two layers adjacent to the ith interface.

In the derivation of Eqs. (6), the coupling between mechanical and electrical fields is not considered to avoid complications and other difficulties like the problem in satisfaction of the interelemental continuity requirement. It has been numerically verified in an earlier work [24] that the effect of this simplification is insignificant on the continuity of transverse shear stresses at the interfaces of piezoelectric and nonpiezoelectric layers.

Using the preceding equations, the strain vector $\{\bar{\varepsilon}\}$ found in Eq. (5) may be expressed in terms of unknown displacement parameters at the reference ($z = 0$) plane and unknown potential and its derivatives at different interfaces as

$$\begin{aligned}&\{\bar{\varepsilon}\}\\ &= \begin{bmatrix}\bar{u}_{,x} & \bar{v}_{,y} & \bar{u}_{,y} + \bar{v}_{,x} & \bar{u}_{,z} + \bar{w}_{,x} & \bar{v}_{,z} + \bar{w}_{,y} & \phi_{,x} & \phi_{,y} & \phi_{,z}\end{bmatrix}^T\\ &= [L]\begin{bmatrix} u_{,x} & v_{,y} & u_{,y} + v_{,x} & w_{,xx} & w_{,yy} & w_{,xy} & \gamma_x & \gamma_{x,x} \\ & \gamma_{x,y} & \gamma_y & \gamma_{y,x} & \gamma_{y,y} & w_{,x} & w_{,y} & \phi_{,x}^1 \\ & \phi_{,y}^1 & \phi_{,z}^1 & \phi_{,x}^2 & \cdots & \cdots & \phi_{,z}^n & \phi_{,x}^{n+1} \\ & \phi_{,y}^{n+1} & \phi_{,z}^{n+1} & & & & & \end{bmatrix}\\ &\text{or} \quad \{\bar{\varepsilon}\} = [L]\{\varepsilon\}\end{aligned} \tag{7}$$

where the elements of $[L]$ are functions of z and unit step functions.

In a similar manner, the displacement components at any point within the plate may be expressed in terms of reference plane parameters as

$$\{\bar{f}\} = \begin{Bmatrix}\bar{u}\\ \bar{v}\\ \bar{w}\end{Bmatrix} = [R]\begin{Bmatrix}u\\ v\\ w\\ \gamma_x\\ \gamma_y\end{Bmatrix} = [R]\{f\} \tag{8}$$

With the preceding equation, the velocity components at any point may be expressed as

$$\frac{\partial}{\partial t}\{\bar{f}\} = \{\dot{\bar{f}}\} = [R]\{\dot{f}\} \tag{9}$$

Now the energy V of the system may be expressed as

$$V = T - U + W = T - U + (W_m + W_e) \tag{10}$$

where T is the kinetic energy, U is the strain energy, W_m is the work done by the applied load, and W_e is the work done by the applied surface charge.

With the help of Eqs. (5) and (7), the strain energy U may be expressed as

$$\begin{aligned}U &= \frac{1}{2}\sum_{k=1}^{n}\iiint\{\bar{\varepsilon}\}^T\left[\bar{Q}^k\right]\{\bar{\varepsilon}\}\,dx\,dy\,dz\\ &= \frac{1}{2}\sum_{k=1}^{n}\iiint\{\varepsilon\}^T[L]^T\left[\bar{Q}^k\right][L]\{\varepsilon\}\,dx\,dy\,dz\end{aligned} \tag{11}$$

Similarly, the kinetic energy T may be expressed with the help of Eq. (9) as

$$\begin{aligned}T &= \frac{1}{2}\sum_{k=1}^{n}\iiint\{\dot{\bar{f}}\}^T\rho_k\{\dot{\bar{f}}\}\,dx\,dy\,dz\\ &= \frac{1}{2}\sum_{k=1}^{n}\iiint\{\dot{f}\}^T[R]^T\rho_k[R]\{\dot{f}\}\,dx\,dy\,dz\end{aligned} \tag{12}$$

where ρ_k is the mass density of the kth layer.

The work done by a distributed transverse load of intensity q may be expressed as

$$W_m = \iint wq\,dx\,dy \tag{13}$$

whereas the work done due to a distributed surface charge s at the ith interface is

$$W_e = \iint \phi^i s\,dx\,dy \tag{14}$$

Now, the in-plane variation of the basic unknowns is represented by finite element approximation. In the present problem, the field variables (basic unknowns) are u, v, w, γ_x, and γ_y for structural deformation whereas $\phi^1, \phi^2, \ldots, \phi^{n+1}$ are those for the electric field. Here, it should be noted that the present plate model requires C^1 continuity of transverse displacement w at the element interfaces because some strain terms [17] contain second-order derivatives of w. This is a well-known problem of plate finite element as mentioned earlier. Keeping this aspect in view, a rectangular element having four nodes at its four corners is developed (Fig. 2). Taking u, v, w, $w_{,x}$, $w_{,y}$, $w_{,xy}$, γ_x, γ_y, and $\phi^1, \phi^2, \ldots, \phi^{n+1}$ as the degrees of freedom at each node, all the field variables except w are interpolated with bilinear interpolation functions, whereas bicubic interpolation functions are used to interpolate w as follows:

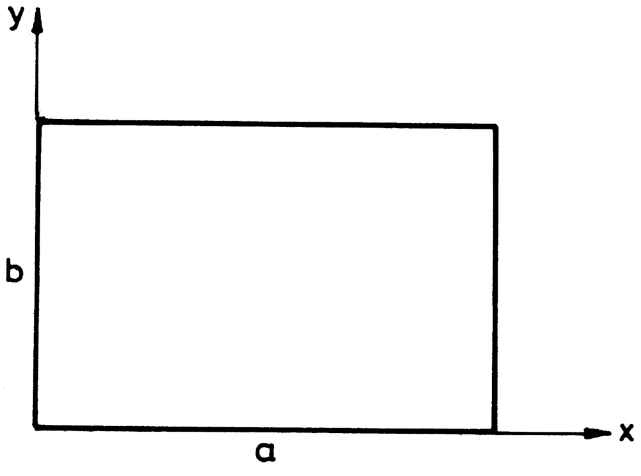

Fig. 2 Geometry of a rectangular plate.

$$u = N_1^l u_1 + N_2^l u_2 + N_3^l u_3 + N_4^l u_4 = \sum_{i=1}^{4} N_i^l u_i = [N^l]\{\delta\}$$

$$v = \sum_{i=1}^{4} N_i^l v_i, \qquad \gamma_x = \sum_{i=1}^{4} N_i^l (\gamma_x)_i, \qquad \gamma_y = \sum_{i=1}^{4} N_i^l (\gamma_y)_i$$

$$\phi^j = \sum_{i=1}^{4} N_i^l \phi_i^j$$

$$w = N_1^c w_1 + N_2^c (w_{,x})_1 + N_3^c (w_{,y})_1 + N_4^c (w_{,xy})_1 + N_5^c w_2 + \cdots + N_{16}^c (w_{,xy})_4 = \sum_{i=1}^{16} N_i^c \delta_i^w = [N^c]\{\delta\} \tag{15}$$

where N_i^l and N_i^c are the bilinear and bicubic interpolation functions, respectively, for ith node. It has ensured C^1 continuity for w and C^0 continuity for the other field variables as desired by the proposed plate model.

With the help of Eq. (15), the vector $\{\varepsilon\}$ as found in Eq. (7) may be expressed in terms of $\{\delta\}$ containing nodal degrees of freedom as

$$\{\varepsilon\} = [B]\{\delta\} \tag{16}$$

where $[B]$ contains interpolation functions N_i^l and N_i^c and their derivatives.

In a similar manner, the vector $\{\dot{f}\}$ found in Eq. (9) may be expressed in terms of $\{\dot{\delta}\}$ as

$$\{\dot{f}\} = [C]\{\dot{\delta}\} \tag{17}$$

With the help of Eqs. (11–14), (16), and (17), Eq. (10) may be expressed as

$$V = \sum_{i=1}^{N} \left(\frac{1}{2}\{\dot{\delta}\}^T [M_e]\{\dot{\delta}\} - \frac{1}{2}\{\delta\}^T [K_e]\{\delta\} + \{\delta\}^T \{R_m\} + \{\delta\}^T \{R_e\} \right) \tag{18}$$

where,

$$[K_e] = \sum_{k=1}^{n} \iiint [B]^T [L]^T [\bar{Q}^k][L][B]\, \mathrm{d}x\, \mathrm{d}y\, \mathrm{d}z \tag{19}$$

$$[M_e] = \sum_{k=1}^{n} \iiint \rho_k [C]^T [R]^T [R][C]\, \mathrm{d}x\, \mathrm{d}y\, \mathrm{d}z \tag{20}$$

$$\{R_m\} = \iint [N^c]^T q\, \mathrm{d}x\, \mathrm{d}y \tag{21}$$

$$\{R_e\} = \iint [N^l]^T s\, \mathrm{d}x\, \mathrm{d}y \tag{22}$$

and N is the total number of elements. The Hamilton's variational principle of dynamics may be applied to Eq. (18) to get the equation of motion of the system. For an element, it may be expressed as

$$[K_e]\{\delta\} + [M_e]\{\ddot{\delta}\} = \{R_m\} + \{R_e\} = \{R\} \tag{23}$$

If the effect of damping is considered, the above equation may be written as

$$[K_e]\{\delta\} + [C_e]\{\dot{\delta}\} + [M_e]\{\ddot{\delta}\} = \{R\} \tag{24}$$

The stiffness matrix $[K_e]$, damping matrix $[C_e]$, mass matrix $[M_e]$, and load vector $\{R\}$ of all the elements are computed and assembled together to form the overall stiffness matrix $[K]$, damping matrix $[C]$, mass matrix $[M]$, and load vector $\{F\}$ of the entire structure where the matrices $[K]$, $[C]$, and $[M]$ are stored in single array following skyline storage technique. With these matrices, the equation of motion of the system may be expressed as

$$[K]\{\Delta\} + [C]\{\dot{\Delta}\} + [M_e]\{\ddot{\Delta}\} = \{F\} \tag{25}$$

After substitution of boundary conditions in the above equation, it is solved directly with the Newmark's β technique of time integration [25].

Before solving the above equation, the degrees of freedom for the electric potential are eliminated from it, as mentioned earlier. The elimination is carried out through static condensation technique, which is convenient to be applied at the element level. This is carried out by partitioning the matrix Eq. (24) in terms of mechanical and electrical components as

$$\begin{bmatrix} [K_{mm}] & [K_{me}] \\ [K_{em}] & [K_{ee}] \end{bmatrix} \begin{Bmatrix} \{\delta_m\} \\ \{\delta_e\} \end{Bmatrix} + \begin{bmatrix} [C_{mm}] & 0 \\ 0 & 0 \end{bmatrix} \begin{Bmatrix} \{\dot{\delta}_m\} \\ \{\dot{\delta}_e\} \end{Bmatrix} + \begin{bmatrix} [M_{mm}] & 0 \\ 0 & 0 \end{bmatrix} \begin{Bmatrix} \{\ddot{\delta}_m\} \\ \{\ddot{\delta}_e\} \end{Bmatrix} = \begin{Bmatrix} \{R_m\} \\ \{R_e\} \end{Bmatrix} \tag{26}$$

Eliminating $\{\delta_e\}$ from the above equation, one obtains

$$[\bar{K}]\{\delta_m\} + [\bar{C}]\{\dot{\delta}_m\} + [\bar{M}]\{\ddot{\delta}_m\} = \{\bar{R}\} \tag{27}$$

where $[\bar{K}] = [K_{mm}] - [K_{me}][K_{ee}]^{-1}[K_{em}]$, $[\bar{C}] = [C_{mm}]$, $[\bar{M}] = [M_{mm}]$, and $\{\bar{R}\} = \{R_m\} - [K_{me}][K_{ee}]^{-1}\{R_e\}$

In the solution of Eq. (25), the nodal displacements vector $\{\delta_m\}$ of an element at any instant of time is extracted from the nodal displacements vector of the whole structure at that time and it may be used to retrieve the corresponding vector $\{\delta_e\}$ for electric potential as

$$\{\delta_e\} = -[K_{ee}]^{-1}[K_{em}]\{\delta_m\} + [K_{ee}]^{-1}\{R_e\} \tag{28}$$

Now the above vector may be partitioned in terms of potential at sensor $\{\phi_s\}$, core $\{\phi_c\}$, and actuator $\{\phi_a\}$ as

$$\{\delta_e\} = \begin{Bmatrix} \{\phi_s\} \\ \{\phi_c\} \\ \{\phi_a\} \end{Bmatrix} \tag{29}$$

For the suppression or control of structural vibration, the sensor voltage is used as feedback to get the potential to be supplied to the actuators as

$$\{\phi_a\} = G\{\phi_s\} \tag{30}$$

where G is defined as gain.

III. Results and Discussion

In this section, the proposed refined hybrid plate model is applied to the solution of numerical examples covering a wide range of features. At the beginning, attempts are made to validate the different components of the present formulation where a problem of static analysis is also considered. Once the performance of the model is tested, it is applied to dynamic response and control of smart sandwich laminates under different conditions.

A. Static Response of a Smart Composite Laminate

A laminated $(p/0/90//0//90/0/p)$ square (axa) plate simply supported at the four edges and subjected to distributed transverse load (static) of intensity $q = q_0 \sin(\pi x/a)\sin(\pi y/a)$ having the peak at the plate center is taken in this example. For surface-bonded piezoelectric layers, the material used is PZT-4 having a thickness of $0.025h$ each, where h is the total thickness of the plate. The material used for the other layers is graphite/epoxy, where the thickness of each of these layers is $0.05h$ except the central layer, which is $0.75h$ thick. The material properties used are

$$\text{PZT-4: } E_{11} = E_{22} = 81.3 \text{ GPa}, \qquad E_{33} = 64.5 \text{ GPa}$$
$$G_{12} = 30.6 \text{ GPa}, \qquad G_{13} = G_{23} = 25.6 \text{ GPa}, \qquad \nu_{12} = 0.329$$
$$\nu_{13} = \nu_{23} = 0.43, \qquad k_{11}/k_0 = k_{22}/k_0 = 1475.0$$
$$k_{33}/k_0 = 1300.0, \qquad k_0 = 8.85 \times 10^{-12} \text{ F/m}$$
$$e_{31} = e_{32} = -5.20 \text{ C/m}^2, \qquad e_{33} = 15.08 \text{ C/m}^2$$
$$e_{24} = e_{15} = 12.72 \text{ C/m}^2$$

$$\text{graphite/epoxy ply: } E_{11} = 132.38 \text{ GPa}$$
$$E_{22} = E_{33} = 10.756 \text{ GPa}, \qquad G_{12} = G_{13} = 5.654 \text{ GPa}$$
$$G_{23} = 3.606 \text{ GPa}, \qquad \nu_{12} = \nu_{13} = 0.24, \qquad \nu_{23} = 0.49$$
$$k_{11}/k_0 = 3.5, \qquad k_{22}/k_0 = 3.0, \qquad k_{33}/k_0 = 3.0$$

To simulate this plate as a sandwich laminate, the material properties of the central thick layer is varied where its values of elastic moduli are expressed as a fraction f of those of thin graphite/epoxy layers. The plate with a thickness ratio a/h of 10 is analyzed for different values of f ranging from 1.0 to 0.02 where the piezoelectric parameters of PZT-4 are taken as zero for the purpose of validation. Values for deflection, in-plane normal stress, and transverse shear stress at important locations of the plate are obtained by the proposed model and the results are presented in Table 1 along with those of elasticity solution of Pagano [26]. The agreement between the results clearly shows the performance of the proposed model and its capability. The analysis is also carried out with the options of HSDT and FSDT of the present formulation and the results obtained are included in Table 1, which shows the inability of these plate theories especially for lower values of f.

Now the problem is studied for a specific value of f (=0.02) where the piezoelectric parameters of PZT-4 are activated and the interface between the piezoelectric layers and the graphite/epoxy layers are grounded. To control the structural deformation, voltage is applied at the plate top surface (actuator) using the voltage generated at the lower surface of the plate (sensor) as feedback. In this case, the analysis is carried out with the full form of the present formulation (all the degrees of freedom are retained) as well as its condensed form (degrees of freedom for the electric potential are eliminated). The values of central deflection obtained for two separate thickness ratios ($a/h = 10$ and 20) and for different combinations of load and voltage are presented in Table 2, which shows that the solution accuracy is not practically affected in the analysis by the condensed model.

The study is carried out with four different mesh sizes, ranging from 4×4 to 12×12, to show the convergence of the present results with mesh refinement.

B. Dynamic Response of a Smart Composite Laminate Under Applied Surface Potential

The problem of a simply supported square laminate $(p/0/90/0/p)$ subjected to electric load in the form of applied voltage $V = V_0 \sin(\pi x/a) \sin(\pi y/a) \sin(\omega t)$ at the plate top surface (actuator), as studied by Ray et al. [27], is considered in this example. The thickness of each surface-bonded piezoelectric layer (PVDF) is 0.1 mm, whereas that of each layer of the cross-ply (0/90/0) laminated core is 2.0 mm. The material properties of the core layers and PVDFs are as follows [26]:

$$\text{core layers: } E_1/E_2 = 25, \qquad E_2 = E_3 = 21.0 \text{ GPa}$$
$$G_{12} = G_{13} = 0.5E_2, \qquad G_{23} = 0.2E_2$$
$$\nu_{12} = \nu_{13} = \nu_{23} = 0.25; \qquad \rho = 800 \text{ N} \cdot \text{s}^2/\text{m}^4$$

$$\text{PVDF layers: } E = 2.0 \text{ GPa}, \qquad \nu = 0.25$$
$$\rho = 100 \text{ N} \cdot \text{s}^2/\text{m}^4, \qquad e_{31} = e_{32} = 0.046 \text{ C/m}^2$$
$$e_{15} = e_{24} = e_{33} = 0.0, \qquad k_{11} = k_{22} = k_{33} = 0.1062 \times 10^{-9} \text{ F/m}$$

The plate is analyzed by the present element with mesh size of 4×4 taking $V_0 = 100$ V, $\omega = 100$ rad/s, and $a/h = 6, 10, 20, 30, 50$ as is used in [3]. Similar to the preceding example, the interfaces between the piezoelectric layers and the core are grounded. The analysis is carried out with different values of time step Δt for a particular case

Table 1 Deflection and stresses of the $p/0/90//0//90/0/p$ plate ($a/h = 10$) under transverse load

Parameter	Method	f					
		1.00	0.50	0.20	0.10	0.05	0.02
w_c [a]	present (4 × 4)	0.80157	1.0629	1.5221	2.1184	3.2095	6.2843
	present (6 × 6)	0.80159	1.0630	1.5225	2.1197	3.2138	6.3070
	present (8 × 8)	0.80160	1.0630	1.5226	2.1201	3.2151	6.3145
	present (12 × 12)	0.80160	1.0630	1.5227	2.1203	3.2161	6.3198
	3-D elasticity [26]	0.80314	1.0644	1.5236	2.1211	3.2171	6.3242
	HSDT (12 × 12) (present)	0.80155	1.0591	1.4710	1.8963	2.4349	3.2215
	FSDT (12 × 12) (present)	0.78303	0.98045	1.1644	1.2456	1.2917	1.3215
σ_x^t [b]	present (4 × 4)	0.38008	0.47108	0.56680	0.63245	0.70772	0.85608
	present (6 × 6)	0.37806	0.46892	0.56539	0.63292	0.71237	0.87386
	present (8 × 8)	0.37734	0.46816	0.56489	0.63308	0.71400	0.88013
	present (12 × 12)	0.37683	0.46761	0.56453	0.63320	0.71517	0.88462
	3-D elasticity [26]	0.37912	0.46930	0.56557	0.63413	0.71653	0.88812
	HSDT (12 × 12) (present)	0.38047	0.46918	0.55587	0.60191	0.63435	0.65962
	FSDT (12 × 12) (present)	0.36832	0.45000	0.51936	0.54744	0.56260	0.57207
τ_{xz}^1 [c]	present (4 × 4)	0.11595	0.14410	0.17547	0.19951	0.23023	0.29707
	present (6 × 6)	0.11666	0.14493	0.17630	0.20012	0.23026	0.29527
	present (8 × 8)	0.11691	0.14523	0.17660	0.20034	0.23027	0.29462
	present (12 × 12)	0.11709	0.14544	0.17681	0.20050	0.23028	0.29416
	3-D elasticity [26]	0.11660	0.14359	0.17017	0.18514	0.19668	0.20515
	HSDT (12 × 12) (present)	0.08529	0.15001	0.32013	0.55486	0.89653	1.4280
	(present)	0.13373	0.11700	0.10039	0.08700	0.07029	0.04478
	FSDT (12 × 12) (present)	0.11386	0.15768	0.20895	0.23577	0.25235	0.26364
		0.17853	0.12361	0.06552	0.03697	0.01978	0.00827

[a] $w_c = 100E_2(\text{Gr/Epoxy})h^3 w/q_0 a^4$ [b] $\sigma_x^t = \sigma_x(a/2, b/2, 0.5h)h^2/q_0 a^2$ [c] $\tau_{xz}^1 = \tau_{xz}(0, b/2, 0.375h)h/q_0 a$

Table 2 Deflection $[100E_2(\mathrm{Gr/Epoxy})h^3w/q_0a^4]$ of the $p/0/90//0//90/0/p$ plate under load and voltage

a/h	Mesh	$q_0 = 1.0$		$q_0 = 1.0, V_0 = 1.0$		$q_0 = 1.0, V_0 = 10.0$		$q_0 = 1.0, V_0 = -1.0$	
		Case 1[a]	Case 2[b]	Case 1	Case 2	Case 1	Case 2	Case 1	Case 2
10	4×4	6.1472	6.1470	26.210	26.212	206.17	206.18	−13.780	−13.781
	6×6	6.1696	6.1695	26.550	26.551	209.36	209.37	−14.074	−14.075
	8×8	6.1770	6.1770	26.669	26.669	210.48	210.49	−14.178	−14.179
	12×12	6.1821	6.1822	26.754	26.754	211.28	211.29	−14.253	−14.253
20	4×4	2.3224	2.3224	6.3124	6.3125	41.840	41.841	−1.5827	−1.5828
	6×6	2.3241	2.3241	6.3721	6.3721	42.421	42.422	−1.6389	−1.6389
	8×8	2.3247	2.3247	6.3931	6.3931	42.626	42.627	−1.6588	−1.6588
	12×12	2.3250	2.3250	6.4081	6.4081	42.773	42.773	−1.6731	−1.6731

[a]Case 1: Full [b]Case 2: Condensed

Table 3 Deflection $w_{c_{\mathrm{normal}}}$ of the $p/0/90/0/p$ plate subjected to applied voltage

Source	$a/h = 6$	$a/h = 10$	$a/h = 20$	$a/h = 30$	$a/h = 50$
Present	−2.915	−6.069	−19.91	−43.16	−122.15
3-D elasticity [26]	−2.945	−6.200	−20.44	−43.97	−119.6
FEM [3]	−2.752	−5.704	−18.65	−39.91	−107.2

$(a/h = 50)$, where $\Delta t = 10$ μs is found to be more than sufficient and it has been applied for all the cases. The maximum values of central deflection

$$(w_{c_{\mathrm{normal}}})\left[= \frac{E_2(\mathrm{core})}{V_0 e_{31}} w(a/2, b/2, 0)\right]$$

obtained in the present analysis are presented in Table 3 along with those obtained from the 3-D elasticity solution [26]. The agreement between the results is found to be very good. Ray et al. [27] have also solved the problem by a finite element model [3] based on single layer plate theory. The results obtained by them are also included in Table 3, which shows that their finite element model [3] is not as accurate as the present model is, as expected. In addition, the time history of the central deflection $w_{c_{\mathrm{normal}}}$ is plotted in Fig. 3 for $a/h = 10$, 20, and 30.

C. Response and Control of a Smart Composite Laminate Under Sudden Release of Load

The dynamic response of a simply supported square laminate $(p/0/90/0/p)$ due to sudden release of a uniformly distributed load (1000 N/m^2) carried by the plate is studied in this example. In this case, the control of dynamic response for different values of gain is also studied. The thickness and material properties of the individual layers as well as the grounding condition are identical to those used in the preceding example. The study is made for $a/h = 10$ and 30. The effect of structural damping is taken into account; the damping matrix is defined in terms of stiffness and mass matrices as $[\mathrm{C_{mm}}] = \alpha[\mathrm{K_{mm}}] + \beta[\mathrm{M_{mm}}]$, where

$$\alpha = 8.0 \times 10^{-7} \text{ rad/s} \quad \text{and} \quad \beta = 2.3 \times 10^3 \text{ s/rad for } a/h = 10$$
$$\text{and} \quad \alpha = 1.0 \times 10^{-6} \text{ rad/s} \quad \text{and}$$
$$\beta = 0.965 \times 10^3 \text{ s/rad for } a/h = 30$$

The analysis is carried out with mesh size of 4×4 and time step of 2.5 μs. The time history of the central deflection

$$w_{c_{\mathrm{normal}}} = \frac{100E_2(\mathrm{core})h^3}{q_0a^4} w$$

for three different values of feedback gains obtained in the present analysis is plotted in Figs. 4 and 5 for $a/h = 10$ and 30, respectively. This problem has also been studied by Samanta et al. [3] by a finite element model based on a single layer plate theory as mentioned in the preceding example. It is expected that the present results will not have very good agreement with those of [3] as explained in the preceding example, but the overall pattern is found to be similar in both the cases.

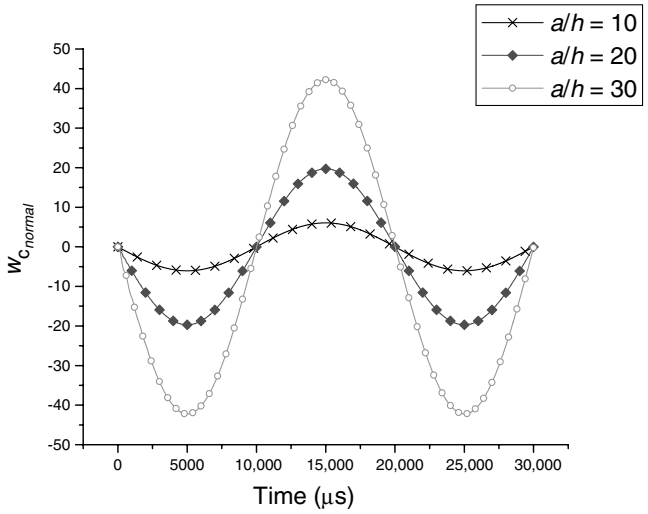

Fig. 3 Response for central deflection of a square $p/0/90/0/p$ plate under sinusoidal voltage.

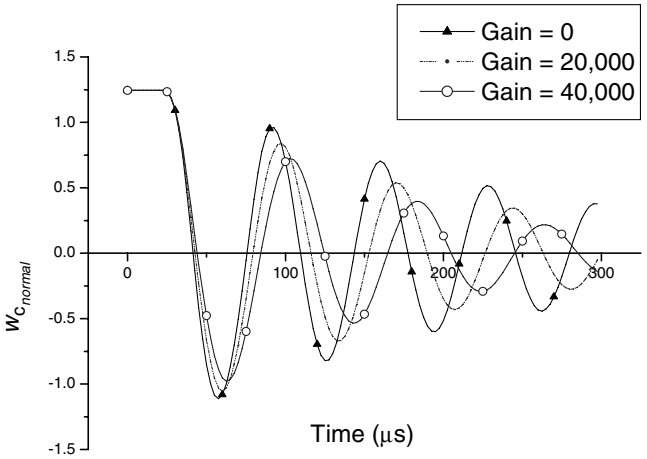

Fig. 4 Response of a $p/0/90/0/p$ plate $(a/h = 10)$ for sudden release of load.

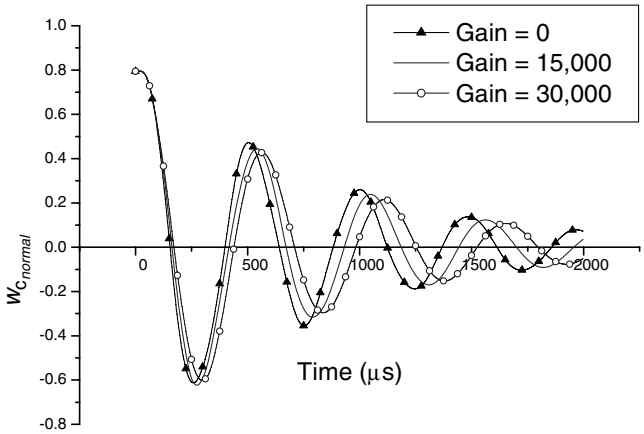

Fig. 5 Response of a $p/0/90/0/p$ plate ($a/h = 30$) for sudden release of load.

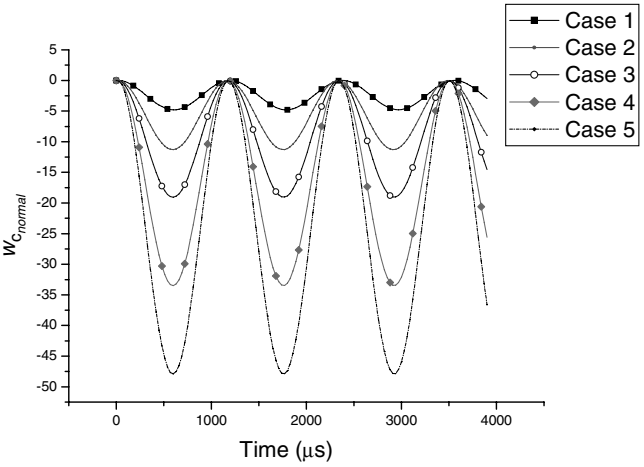

Fig. 6 Response of a smart plate for voltage applied at different piezoelectric layer.

D. Response of Smart Composite Laminates with Embedded Piezoelectric Layers Subjected to Suddenly Applied Surface Potential

In most of the studies on smart laminates, it is found that the formulation is restricted to handle surface-bonded piezoelectric layers only. As the present formulation is free from that limitation and is capable of modeling a smart laminate with any number of piezoelectric layers placed anywhere inside the plate thickness, a problem of that type is considered in this example. The plate is a simply supported square laminate having three different ply arrangements depending on the placement of the embedded piezoelectric layers, and they are PA_1: $p/0/90/0/p/90//90/p/0/90/0/p$, PA_2: $p/0/90/p/0/90//90/0/p/90/0/p$, and PA_3: $p/0/p/90/0/90//90/0/90/p/0/p$. The thickness ratio a/h of the plate is taken as 10 ($h = 0.1$ m), where the thickness h_p of four piezoelectric layers is $0.20h$ ($4 \times 0.05h$), and the rest of the thickness is equally shared by the fiber reinforced composite layers. The material properties are identical to those in the second example. Under the action of suddenly applied electric potential $[V = V_0 \sin(\pi x/a) \sin(\pi y/a)]$ at the different surfaces of the piezoelectric layers, the dynamic response of the plate is studied for five different cases as follows:

Case 1: plate PA_1 is subjected to electric potential ($V_0 = 100$ V) at the top surface of upper embedded piezoelectric layer and that with $V_0 = -100$ V at the bottom surface of lower embedded piezoelectric layer. The other surfaces of these two piezoelectric layers are grounded.

Case 2: plate PA_2 with applied potential and grounding condition like that of case 1.

Case 3: plate PA_3 with applied potential and grounding condition like that of case 1.

Case 4: case 3 with additional electric potential ($V_0 = 100$ V) at the top surface of the uppermost piezoelectric layer where its other side is grounded.

Case 5: case 4 with additional electric potential ($V_0 = -100$ V) at the plate bottom surface of the lowermost piezoelectric layer where its other side is grounded.

In all the cases, the analysis is carried out with mesh size of 4×4 and $\Delta t = 30.0$ μs; the time history obtained for the central deflection

$$w_{c_{\text{normal}}} = \frac{E_2(\text{core})}{100 e_{31}} w$$

is presented in Fig. 6. The figure shows that the location of piezoelectric layers has a telling effect on the actuation power generated by a given applied electric potential. The actuation, in fact, gets enhanced with the increase in distance of the piezoelectric layers from the plate neutral plane. Thus, to have a better actuation, the surface-bonded and/or neighboring embedded piezoelectric layers should be used as actuators, whereas an embedded piezoelectric layer placed anywhere inside the laminate may be used as sensor.

The effect of boundary condition on the response characteristics is studied by taking the plate PA_3, which is subjected to electric potential V only at the plate top surface, whereas the bottom surface of the uppermost piezoelectric layer is grounded. The different boundary conditions taken are 1) SSSS: all the edges are simple supported; 2) CCCC: all the edges are clamped; and 3) SCSC: two opposite edges are simple supported and the other edges are clamped. For these three cases, the time history for the normalized central deflection $w_{c_{\text{normal}}}$ obtained with the same time step and mesh size as earlier is presented in Fig. 7.

E. Response and Control of Smart Double Core Sandwich Laminates Subjected to Suddenly Applied Transverse Load

The dynamic response of a simply supported square sandwich laminate ($a/h = 10$) with surface-bonded piezoelectric layers is studied in this example. For this purpose, two different stacking sequences are taken: case 1: $p/0/90/0/90//C/C//0/90/90/0/p$ and case 2: $p/0/90//C/0/90/0/90/C//90/0/p$. The materials used for surface-bonded piezoelectric layers and the cross-ply laminated stiff sheets ($0/90\cdots$) are PZT-4 and graphite/epoxy, respectively (material properties are given in the first example). A low strength isotropic material ($E = 6.89 \times 10^6$ GPa and $G = 3.45 \times 10^6$ GPa) is used for the core layers /C/. The density ρ for each of these three types of material is taken as 1.0 $\text{N} \cdot \text{s}^2/\text{m}^4$. The

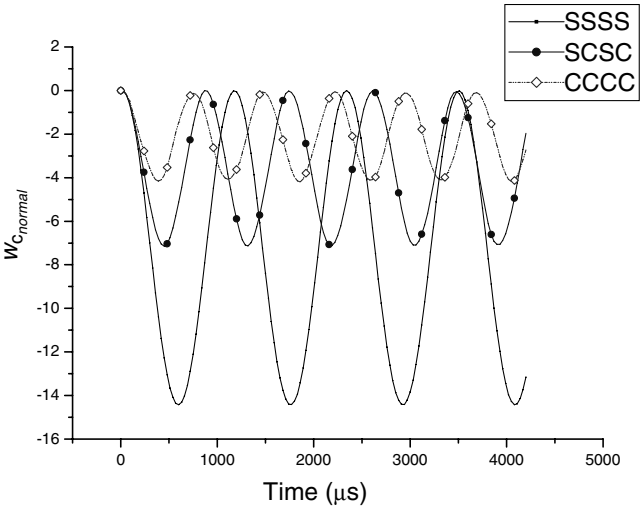

Fig. 7 Effect of boundary conditions on response of a $p/0/p/90/0/90//90/0/90/p/0/p$ plate.

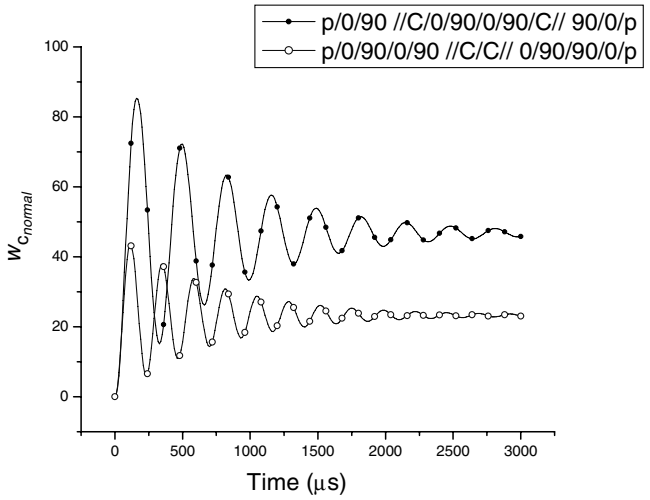

Fig. 8 Effect of core layer placement on response of a smart sandwich plate.

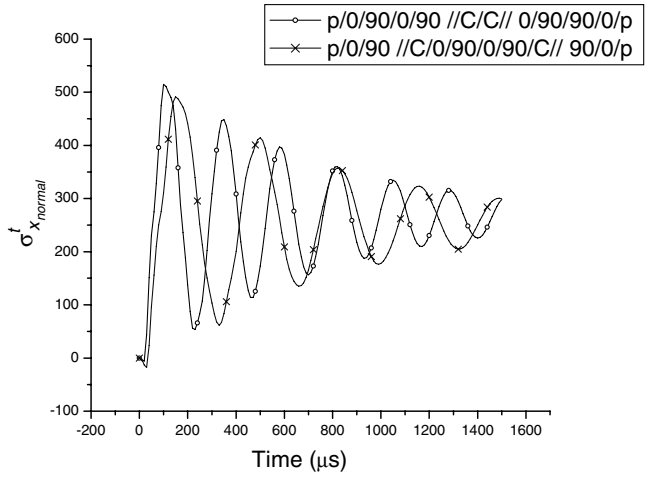

Fig. 9 In-plane normal stress of a smart sandwich plate ($a/h = 10$).

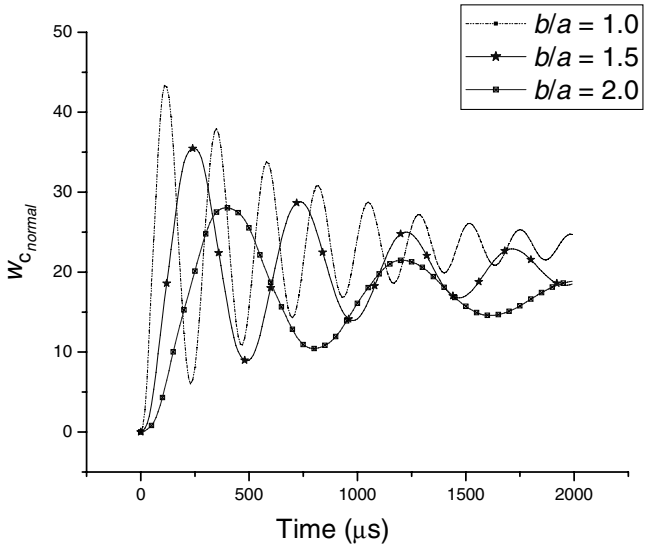

Fig. 10 Effect of aspect ratio on response of a $p/0/90/0/90//C/C//0/90/90/0/p$ sandwich plate ($a/h = 10$).

thickness of each piezoelectric layer, each ply of the cross-ply laminates, and each core layer is $0.05h$, $0.05h$, and $0.25h$, respectively. The interfaces between the piezoelectric layers and graphite/epoxy (Gr/Epoxy) layers are grounded. In this case, the effect of structural damping is considered in a similar manner as taken earlier. Under the action of suddenly applied uniformly distributed transverse load, the plate is analyzed with mesh size of 4×4 and time step of 30 μs. The time histories for the deflection $w_{c_{\text{normal}}}$ and top fiber normal stress $\sigma^t_{x_{\text{normal}}}$ obtained at the plate center are presented in Figs. 8 and 9, respectively, for both the stacking sequences. The figures show that the placement of the core inside the plate has a significant effect on the dynamic response especially in terms of the deflection of the plate. To study the effect of aspect ratio, the plate considered in case 1 is reanalyzed for three different aspect ratios ($b/a = 1.0$, 1.5, and 2.0) in a similar manner and the response for central deflection $w_{c_{\text{normal}}}$ obtained is plotted in Fig. 10. The deflection and extreme fiber normal stress are normalized as follows:

$$w_{c_{\text{normal}}} = \frac{100E_2(\text{Gr/Epoxy})h^3}{q_0 a^4} w(a/2, b/2, 0) \quad \text{and}$$

$$\sigma^t_{x_{\text{normal}}} = \frac{h^2}{q_0 a^2} \sigma_x(a/2, b/2, h/2)$$

The response of a plate, having stacking sequence as defined in case 2 and aspect ratio $b/a = 2.0$, subjected to a uniformly distributed load with time variation as shown in Fig. 11a, is studied with mesh size 4×4 and time step of 25 μs. The response is controlled by applying voltage at the plate top surface, whereas the voltage generated at the plate bottom is taken as feedback to get the actuation voltage with an appropriate gain. For three different values of gain, the time history of the central deflection $w_{c_{\text{normal}}}$ is plotted in Fig. 11b.

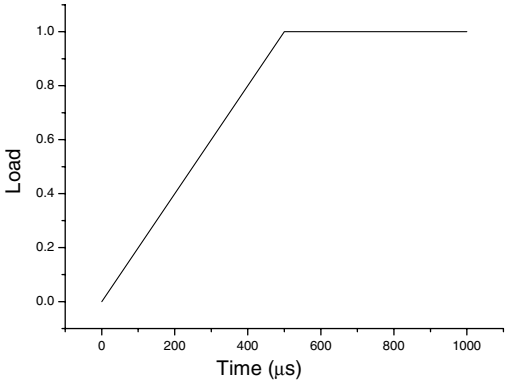

a) Time history of the uniformly distributed pulse load

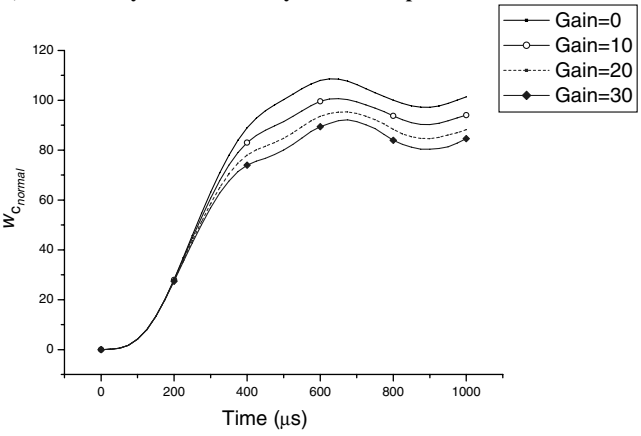

b) Time history of the central deflection of the sandwich plate

Fig. 11 Response of a $p/0/90//C/0/90/0/90/C//90/0/p$ plate ($a/h = 10$; $b/a = 2$) subjected to a pulse load.

IV. Conclusions

The dynamic response and its control of composite and sandwich laminates with surface-bonded as well as embedded piezoelectric layers are studied in this paper. A refined hybrid plate theory is recommended for the modeling of the structure that involves a coupled electromechanical field problem. This plate theory demonstrates piecewise parabolic variation of in-plane displacements and it ensures transverse shear stress continuity at the layer interfaces, as well as stress-free conditions at plate top and bottom surfaces. The plate theory is capable of representing any arbitrary through-thickness variation of electric potential that is caused by the presence of embedded piezoelectric layers. Interestingly, the plate theory having such capabilities effectively retains unknowns at the reference plane only. For finite element implementation of this plate theory, C^1 continuity of transverse displacement is required at the element interfaces. As this requirement cannot be fulfilled by most of the existing elements, a new four-noded rectangular element is developed in the present study where this continuity condition is fully ensured. Numerical examples are solved by this finite element model, which shows that its performance is very good vis-à-vis the 3-D elasticity solution. Finally, the model is applied to a number of problems obtained by varying different parameters. Effect of placement of the embedded piezoelectric layers is studied and it is observed that it has a telling effect on the deformation characteristics. Similarly, the positioning of the low strength core in a smart sandwich laminate is found to have a significant effect on the dynamic response of transverse displacement.

References

[1] Hagood, N. W., Chang, W. H., and Von, F. A., "Modeling of Piezoelectric Actuator Dynamics for Active Structural Control," *AIAA/ASME/ASCE/AHS/ASC 31st Structures, Structural Dynamics, and Material Conference*, NASA, Washington, DC, 1990, pp. 2242–2256.

[2] Ray, M. C., Bhattacharya, R., and Samanta, B., "Static Analysis of an Intelligent Structure by the Finite Element Method," *Computers and Structures*, Vol. 52, No. 4, 1994, pp. 617–631.

[3] Samanta, B., Ray, M. C., and Bhattacharya, R., "Finite Element Model for Active Control of Intelligent Structures," *AIAA Journal*, Vol. 34, No. 9, 1996, pp. 1885–1893.

[4] Kim, J., Varadan, V. V., and Varadan, V. K., "Finite Element Modelling of Structures Including Piezoelectric Active Devices," *International Journal for Numerical Methods in Engineering*, Vol. 40, No. 5, 1997, pp. 817–832.

[5] Allik, H., and Hughes, T. J. R., "Finite Element Method for Piezoelectric Vibration," *International Journal for Numerical Methods in Engineering*, Vol. 2, No. 2, 1970, pp. 151–157.

[6] Tzou, H. S., and Tseng, C. I., "Distributed Piezoelectric Sensor/Actuator Design for Dynamic Measurement/Control of Distributed Parameter Systems: A Piezoelectric Finite Element Approach," *Journal of Sound and Vibration*, Vol. 138, No. 1, 1990, pp. 17–34.

[7] Sze, K. Y., and Yao, L. Q., "Modeling Smart Structures with Segmented Piezoelectric Sensors and Actuators," *Journal of Sound and Vibration*, Vol. 235, No. 3, 2000, pp. 495–520.

[8] Heyliger, P. R., Ramirez, G., and Saravanos, D. A., "Coupled Discrete-Layer Finite-Element Models for Laminated Piezoelectric Plates," *Communications in Numerical Methods in Engineering*, Vol. 10, No. 12, 1994, pp. 971–981.

[9] Saravanos, D. A., Heyliger, P. R., and Hopkins, D. A., "Layerwise Mechanics and Finite Element Model for the Dynamic Analysis of Piezoelectric Composite Plates," *International Journal of Solids and Structures*, Vol. 34, No. 3, 1997, pp. 359–378.

[10] Srinivas, S., "A Refined Analysis of Composite Laminates," *Journal of Sound and Vibration*, Vol. 30, No. 4, 1973, pp. 495–507.

[11] Toledano, A., and Murakami, H., "Composite Plate Theory for Arbitrary Laminate Configurations," *Journal of Applied Mechanics*, Vol. 54, No. 1, 1987, pp. 181–189.

[12] Li, X., and Lue, D., "An Improved Shear Stress Continuity Theory for Both Thin and Thick Composite Laminates," *Journal of Applied Mechanics*, Vol. 59, No. 3, 1992, pp. 502–509.

[13] Robbins, D. H., and Reddy, J. N., "Modeling of Thick Composites Using a Layer-Wise Laminate Theory," *International Journal for Numerical Methods in Engineering*, Vol. 36, No. 4, 1993, pp. 655–677.

[14] Mitchell, J. A., and Reddy, J. N., "A Refined Hybrid Plate-Theory for Composite Laminates with Piezoelectric Laminae," *International Journal of Solids and Structures*, Vol. 32, No. 16, 1995, pp. 2345–2367.

[15] Saravanos, D. A., "Coupled Mixed-Field Laminate Theory and Finite Element for Smart Piezoelectric Composite Shell Structure," *AIAA Journal*, Vol. 35, No. 8, 1997, pp. 1327–1333.

[16] Sheikh, A. H., Topdar, P., and Halder, S., "An Appropriate F. E. Model for Through Thickness Variation of Displacement and Potential in Thin/Moderately Thick Smart Laminates," *Composite Structures*, Vol. 51, No. 4, 2001, pp. 401–409.

[17] Di Sciuva, M., "A Refined Transverse Shear Deformation Theory for Multilayered Anisotropic Plates," *Atti della Accademia delle Scienze di Torino*, Vol. 118, No. 1, 1984, pp. 279–295.

[18] Lue, D., and Li, X., "An Overall View of Laminate Theories Based on Displacement Hypothesis," *Journal of Composite Materials*, Vol. 30, No. 14, 1996, pp. 1539–1560.

[19] Bhaskar, K., and Varadan, T. K., "Refinement of Higher Order Laminated Plate Theories," *AIAA Journal*, Vol. 27, No. 12, 1989, pp. 1830–1831.

[20] Di Sciuva, M., "Multilayered Anisotropic Plate Models with Continuous Interlaminar Stress," *Computers and Structures*, Vol. 22, No. 3, 1992, pp. 149–167.

[21] Lee, C. Y., and Liu, D., "Interlaminar Shear Stress Continuity Theory for Laminated Composite Plates," *AIAA Journal*, Vol. 29, No. 11, 1991, pp. 2010–2012.

[22] Cho, M., and Parmerter, R. R., "Efficient Higher Order Plate Theory for General Lamination Configurations," *AIAA Journal*, Vol. 31, No. 7, 1993, pp. 1299–1308.

[23] Reddy, J. N., "A Simple Higher-Order Theory for Laminated Composites," *Journal of Applied Mechanics*, Vol. 51, No. 2, 1984, pp. 745–752.

[24] Topdar, P., Chakraborti, A., and Sheikh, A. H., "An Efficient Hybrid Plate Model for Analysis and Control of Smart Sandwich Laminates," *Computer Methods in Applied Mechanics and Engineering*, Vol. 193, Nos. 42–43, 2004, pp. 4591–4610.

[25] Bathe, K. J., *Finite Element Procedures*, Prentice–Hall, Upper Saddle River, NJ, 1996.

[26] Pagano, N. J., "Exact Solutions for Rectangular Bi-Directional Composites and Sandwich Plates," *Journal of Composite Materials*, Vol. 4, No. 1, 1970, pp. 20–34.

[27] Ray, M. C., Bhattacharya, R., and Samanta, B., "Exact Solutions for Dynamic Analysis of Composite Plates with Distributed Piezoelectric Layers," *Computers and Structures*, Vol. 66, No. 6, 1998, pp. 737–743.

B. Sankar
Associate Editor